Glia

WILEY

GLIA

RESEARCH ARTICLE OPEN ACCESS

Early Developmental Neuronal Activity Impacts Oligodendrocyte Differentiation Through AMPA Receptors

Tessa E. Allen[1,2] | Graham Peet[1,2] | Luis E. Gomez Wulschner[1,3] | Won Chan Oh[1,3] | Wendy B. Macklin[1,2]

[1]Neuroscience Graduate Program, University of Colorado, Anschutz Medical Campus, Aurora, Colorado, USA | [2]Cell and Developmental Biology, University of Colorado, Anschutz Medical Campus, Aurora, Colorado, USA | [3]Department of Pharmacology, University of Colorado, Anschutz Medical Campus, Aurora, Colorado, USA

Correspondence: Wendy B. Macklin (wendy.macklin@cuanschutz.edu)

Received: 31 October 2025 | **Revised:** 10 March 2026 | **Accepted:** 31 March 2026

Keywords: AMPA receptor | development | neuronal activity | neuron–glia interactions | oligodendrocyte | oligodendrogenesis

ABSTRACT

Oligodendrocytes produce myelin, a lipid-rich membrane that wraps neuronal axons in the central nervous system to provide metabolic and trophic support and allow for saltatory conduction. Developation requires precisely timed and localized neuron-oligodendrocyte communication. In the mature brain, neuronal activity promotes oligodendrocyte precursor cell (OPC) proliferation and differentiation, but how OPCs respond to neuronal activity in early brain development, before the onset of myelination, is less well characterized. Here, we investigate how glutamatergic neuronal activity regulates early developmental oligodendrocyte maturation in the olfactory system, somatosensory cortex, and corpus callosum in mice. We find that decreased neuronal activity increases oligodendrocyte differentiation in early development, both in a sensory deprivation model and when using in vivo chemogenetics. Conversely, enhanced neuronal activity in early development reduces oligodendrocyte differentiation. Additionally, single-cell RNA sequencing revealed transcriptional changes in oligodendrocytes when neuronal activity was reduced, including upregulation of glutamate receptor gene expression and pathways relating to synapse development. Finally, using ex vivo cortical slice culture, we identify AMPAR signaling as a critical regulator of the later steps of oligodendrocyte maturation, but not the initiation of differentiation.

1 | Introduction

Oligodendrocytes are the myelinating cells in the central nervous system, providing neurons with metabolic and trophic support and enabling saltatory action potential propagation. Oligodendrocyte progenitor cell (OPC) differentiation and myelination during development require precise spatial and temporal regulation through bidirectional communication between OPCs and neuronal axons, yet this important developmental signaling is not well understood (Thornton and Hughes 2020). Several studies have shown that adult neuronal activity promotes oligodendrocyte proliferation and differentiation (oligodendrogenesis) (Foster et al. 2019). In early development, however, when OPCs are rapidly proliferating and prior to normal developmental myelination, the relationship between oligodendrocytes and neurons remains largely unclear.

In the mouse olfactory system, the lateral olfactory tract (LOT) is one of the earliest white matter tracts to develop in the central nervous system (CNS), as the relay of olfactory information is critical for early mouse development (Logan et al. 2012). Mitral cells and tufted cells in the olfactory bulb send axons to form the LOT as early as E11, and robust myelination of this tract begins around P7 (Foran and Peterson 1992; Walz et al. 2006). Our lab and others have shown that chronic suppression of neuronal activity in adult mouse models leads to decreased oligodendrogenesis and hypomyelination of the adult LOT (Collins et al. 2018;

George et al. 2022). Here, we use this system to address how neuronal activity influences oligodendrogenesis in early development, studying the LOT prior to active myelination.

In mouse cortical development, cortical projection neurons begin to extend axons contralaterally to form the corpus callosum around embryonic day (E) 15 (Rash and Richards 2001). During the first week of postnatal development, there is extensive early axonal exuberance followed by dynamic circuit refinement (De León Reyes et al. 2020). In similar developmental timing, OPCs differentiate from neural stem cell-derived radial glia in the brain starting at E12.5 (Cristobal and Lee 2022). They are abundant in the corpus callosum by postnatal day (P) 0, and begin to populate the cortex at birth (Zheng et al. 2018). In the corpus callosum, OPCs start to differentiate into premyelinating oligodendrocytes around postnatal day (P) 7, and robust myelination begins around P14 (Dawson et al. 2003). Thus, during the first postnatal week, axons are highly active, yet unmyelinated. Indeed, one study showed that sensory deprivation by whisker plucking for the first five postnatal days causes increased oligodendrogenesis in the deprived region of the barrel cortex (Mangin et al. 2012). Similarly, early monocular deprivation in mice increases oligodendrogenesis in cortex (Etxeberria et al. 2016). We hypothesized that before axons are physiologically ready for myelination, the influence of neuronal activity on oligodendrogenesis is different than during active myelination. The current study aims to define how neuronal activity alone regulates oligodendrogenesis before the onset of developmental myelination.

Glutamatergic signaling from neurons to OPCs and oligodendrocytes regulates oligodendroglial maturation and function in the adult central nervous system (CNS). Glutamate signals through various ionotropic and metabotropic receptors, including receptors activated by α-amino-3-hydroxy-5-methyl-4-isoxazolepropionic acid (AMPARs), which are expressed by oligodendrocytes and their precursors (De Biase et al. 2010), among other cells. AMPARs are present in OPCs across species early in development, suggesting that glutamatergic signaling plays an important role in developmental oligodendrogenesis and myelination (Piller et al. 2021; Wosik et al. 2004; McDonald et al. 1998), although their impact is debated. In vitro studies show that AMPAR stimulation inhibits OPC proliferation and differentiation (Gallo et al. 1996; Yuan et al. 1998; Fannon et al. 2015), and both in vitro and in vivo studies show it increases OPC migration (Piller et al. 2021; Harlow et al. 2015; Gudz et al. 2006). Conversely, AMPAR-mediated glutamatergic signaling on OPCs stimulates oligodendrogenesis in vivo and promotes myelination in later development and adulthood (Gallo et al. 1996; Chen et al. 2018; Kougioumtzidou et al. 2017). An important caveat is that these published in vivo studies mostly examine glutamatergic signaling in adulthood or in late development, after robust myelination has begun. The effects of glutamatergic transmission prior to this developmental myelination period have not been studied; thus, how glutamatergic neuronal activity regulates OPCs and oligodendrocytes in the early developmental environment remains unclear. Here, we investigate the role of glutamatergic neuronal activity with a focus on the contribution of oligodendroglial AMPARs to OPC differentiation in early postnatal development.

2 | Methods

2.1 | Animals

All animal experiments were performed with approval from the Institutional Animal Care and Use Committee at University of Colorado, Anschutz Medical Campus. For DREADD experiments, *Neurod6*$^{tm1(cre)Kan}$ (NexCre+/−) (Goebbels et al. 2006) mice were crossed to WT *C57BL/6J* mice and genotyped. Mice were sacrificed via perfusion for immunohistochemistry (IHC) or decapitation for electrophysiology at P7 or P8 as indicated. Unilateral Naris Occlusion (UNO) mice were sacrificed via perfusion at P5. For single cell RNASeq (scRNAseq) experiments, NexCre+/− mice were crossed to WT *C57BL/6J* mice and genotyped. After DREADD/CNO exposure (see in vivo DREADD injections), P8 mice were anesthetized with isoflurane, sacrificed via decapitation, and processed for single cell analyses (see below). For ex vivo cortical slice culture experiments, WT or NexCre+/− mice were sacrificed at P4 by decapitation. Both male and female mice were used for all in vivo and ex vivo experiments. Mouse weights were recorded daily to monitor any changes in health compared to litter matched controls, and no differences were noted (data not shown). All animals were treated and handled equivalently independent of experimental conditions.

2.2 | Unilateral Naris Occlusion

Unilateral naris occlusion (UNO) was performed as previously described (van der Linden et al. 2020). Briefly, P0 pups were cryoanesthetized and then immediately subjected to electrocautery for 1 s on the right nostril under a dissecting microscope. During electrocautery, care was taken to avoid contact of the electrocautery unit with any non-superficial tissues. Upon perfusion, scar formation over the right nostril was confirmed.

2.3 | In Vivo DREADD Injections

Intracranial injections were performed according to our previous study (Ogelman et al. 2024). Briefly, adeno-associated viruses (AAVs) were injected by hand. Neonates (P0–1) were cryoanesthetized, and following cessation of movement, a solution of recombinant AAVs (7×10^{12} viral copies/mL) (Addgene) was injected bilaterally into layer 2/3 of the somatosensory cortex using a pulled glass needle (30–40 μm) (Oh et al. 2021). The needle was held perpendicular to the skull surface during insertion to a depth of approximately 200–300 μm. Once the needle was in place, viral solution (1 μL) was manually injected (Microdispenser, VWR) into each hemisphere. AAVs included pAAV-hSyn-DIO-hM4D(Gi)-mCherry(Gi-DREADD) (Addgene) or pAAV-hSyn-DIO-hM3D(Gq)-mCherry (Gq-DREADD) (Addgene). Litter and age-matched control animals (NexCre−) received the same amount of AAV solution. After injection, pups were placed on a warming pad for recovery (15 min) and

returned to the home cage (Oh et al. 2016). All experimental and control animals were handled equivalently.

2.4 | In vivo clozapine N-oxide (CNO) and 5-Ethynyl-2-deoxyuridine (EdU) administration

Oral CNO administration was performed according to previous studies (Schalbetter et al. 2021). Briefly, CNO was delivered by carefully handling pups and using a pipette to feed pups orally. CNO (1 mg/kg) was administered twice daily (Oh et al. 2021; Schalbetter et al. 2021; Pati et al. 2020). Litter and age-matched controls received the same concentration of CNO. For EdU administration, 5 μg/g EdU was administered IP once daily from P5–P7.

2.5 | Cortical Explant Culture

300 μm thick cortical slices from P4 WT or NexCre+/− mice were prepared (Stoppini et al. 1991). Brains were dissected in carbogenated dissection media (0.5 mL 1 M $CaCl_2$, 2.5 mL 1 M $MgCl_2$, 0.9 g Glucose, 0.149 g KCl (or 2 mL of 1 M KCl), 1.09 g $NaHCO_3$ (Sodium bicarbonate), 40 g Sucrose, 1 mL 0.5% phenol red, dH_2O to 500 mL, sterile filtered) and cultured in culture media (170 mL dH_2O, 2.1 g MEM, 50 mL Horse serum, 1.25 mL 200 mM L-glutamine, 0.25 mL $CaCl_2$, 0.5 mL $MgSO_4$, 0.58 g D-glucose, 0.11 g $NaHCO_3$ (sodium bicarbonate), 1.79 g HEPES, 0.012 mL 25% Ascorbic acid, 0.25 mL 1 mg/mL Insulin. Osmolality between 317 and 323, pH 7.28, Sterile filtered). Culture media was changed every 48 h until 6DIV when treatment was started. For tetrodotoxin (TTX) experiments, 1 μM TTX in media or 1 μM TTX + 50 μM AMPA or media alone was bath applied to the slices for 48 h. The slices were then fixed in 4% paraformaldehyde (PFA) in phosphate buffered saline (PBS) for 20 min and stained for oligodendrocyte lineage markers. For DREADD experiments, immediately after plating from P4 brains, 1 μL Gi-DREADD or control pAAV-hSyn-mCherry (mCh) was pipetted on the surface of each slice. At 6DIV, 1 μM CNO alone in culture media; 1 μM CNO + 100 μM NBQX in culture media or 1 μM CNO + 50 μM AMPA in culture media was bath applied to the appropriate slices. Doses of culture media with 100 μL 1 μM CNO alone; 1 μM CNO + 100 μM NBQX or 1 μM CNO + 50 μM AMPA were spiked in at 24 h. At 48 h, slices were fixed in 4% PFA/PBS for 20 min and stained for oligodendrocyte lineage markers. Media alone was compared to 48 h treatment of CNO, and no differences in oligodendrocyte differentiation markers were noted (Figure S4).

2.6 | Acute Slice Electrophysiology

Mice were sacrificed by decapitation at P7–8. The brain was removed from the skull and rapidly placed in ice-cold cutting solution containing (in mM): 215 sucrose, 20 glucose, 26 $NaHCO_3$, 4 $MgCl_2$, 4 $MgSO_4$, 1.6 NaH_2PO_4, 1 $CaCl_2$, and 2.5 KCl. Cortical slices (300 μm thick) were prepared using a VT1000S (Leica) vibrating microtome. Slices were incubated at 32°C for 30 min in a holding chamber containing 50% cutting solution and 50% artificial cerebrospinal fluid (ACSF) containing (in mM): 127 NaCl, 25 $NaHCO_3$, 25 D-glucose, 2.5 KCl, 1.25 NaH_2PO_4, 2 $CaCl_2$, and 1 $MgCl_2$. After 30 min, this solution was replaced with ACSF at room temperature. Slices were allowed to recover for at least 1 h in ACSF before recording. After recovery, slices were transferred to a submersion type, temperature-controlled recording chamber (TC-324C, Warner Instruments) and perfused with ACSF. All solutions were equilibrated for at least 30 min with 95% O_2/5% CO_2 (Ogelman et al. 2024). Whole-cell recordings (electrode resistance, 5–8 MΩ; series resistance, 20–40 MΩ) were performed at 30°C on visually identified, mCherry+ (Gi or Gq) cortical layer 2/3 pyramidal neurons within 40 μm of the slice surface of acute slices (P7-8) using a MultiClamp 700B amplifier (Molecular Devices). To determine the effect of short-term bath application of Clozapine N-Oxide (CNO, < 60 min) on neuronal excitability following DREADDs expression, resting membrane potentials were recorded in current-clamp mode using potassium-based internal solution (in mM: 136 K-gluconate, 10 HEPES, 17.5 KCl, 9 NaCl, 1 $MgCl_2$, 4 Na_2-ATP, 0.4 Na-GTP, and ~300 mOsm, ~pH 7.26) at 30°C in ACSF containing 2 mM Ca^{2+} and 1 mM Mg^{2+} (Ogelman et al. 2024). Additionally, rheobase of mCherry+ neurons was analyzed in response to 300-msec step current injections (5-pA increments) before and after bath application of 1 μM CNO.

2.7 | Immunohistochemistry

Mice were given an intraperitoneal injection of Fatal Plus (Vortech Pharmaceuticals). Intracardial perfusion was performed using PBS followed by 4% PFA/PBS. Tissues were dissected and then post-fixed in 4% PFA/PBS overnight and transferred to cryoprotect solution (30% sucrose in PBS). Brains were cryosectioned into 30 μm free-floating sections and stored at 4°C in 0.1% Sodium azide solution (Azide and PBS). Before staining, antigen retrieval was performed in 10 mM sodium citrate (pH 6.0) for 10 min at 65°C (550 W), in a Pelco Biowave Pro. Sections were permeabilized in 0.3% Triton-X in PBS for 1 h at room temperature. All primary antibodies were incubated for 3 days at 4°C in 0.1% Triton-X in PBS. The following antibodies and concentrations were used: PDGFRα (R&D Systems AF1062) 1:500; BCAS1 (Santa Cruz sc-136342) 1:500; CC1 (Calbiochem OP80) 1:500; Olig2 (Millipore MABN50) 1:500; mCh (Aves mCherry-0100) 1:1000; PLP1 (AA3 rat monoclonal) (Yamamura et al. 1991) 1:1000; TCF4/TCF7L2 (Cell Signaling C48H11) 1:500. Sections were rinsed for 15 min in PBS and then transferred to secondary antibodies. All secondary antibodies were used at a concentration of 1:1000 in 0.1% Triton-X in PBS and incubated 2 h at room temperature. Sections were rinsed in PBS and then mounted and cover-slipped with Fluoromount-G (ThermoFisher). For the lateral olfactory tract (LOT), images of the entire tract were tiled. For the olfactory bulb (OB), images of the entire OB were tiled. For the cortex, sample images were captured in cortical layer 4 (L4), no further than 500 μm from midline. For the corpus callosum, images were captured at midline. At least three sections per mouse were imaged and analyzed.

2.8 | Image Acquisition and Analysis

Fluorescent images were taken on a Leica DMi8 Stellaris 5 confocal microscope using a 40× oil immersion objective. For each

antibody panel, all microscopy settings were kept constant to maintain consistent and comparable images. Cell counts using fluorescent images were collected by blinded investigators and quantified manually. Intensities of each channel were kept constant across animals to maintain consistent identification of positive cells. Three sections from each animal were averaged.

2.9 | Single-Cell RNA Sequencing

Oligodendrocyte lineage cells were collected from P8 Gi-DREADD injected and CNO treated NexCre+/− and WT controls (Khandker et al. 2022). Briefly, the cortex and corpus callosum were dissected and pooled from three NexCre+/− and two WT littermate P8 pups that were equally treated with Gi-DREADD and CNO as above. The brains were minced and cells dissociated using papain (Worthington Biochemical). Oligodendrocytes were isolated using PDGFRα and O4-positive selection magnetic microbeads (Miltenyi). Transcriptomic libraries were captured using the 10× Chromium controller using V3 chemistry with 3′ selection (10× Genomics). Samples were sequenced to a depth of 50,000 reads per cell by the CU Anschutz Genomics Shared Resource. Sample demultiplexing, barcode processing, and alignment were performed using Cell Ranger (10× Genomics). Processed data were analyzed in R using Seurat version 5.1.0 (Hao et al. 2024; R Core Team 2021). For initial quality control, cells containing fewer than 3000 detected genes and more than 10% percent mitochondrial transcripts were excluded from subsequent analysis. The contribution of the percentage mitochondrial gene reads to variance between cells was regressed out during data normalization and scaling. Unsupervised clustering was performed using a resolution of 0.2 in a UMAP embedding space, also used for visualization. To annotate clusters, the differentially expressed gene lists resulting from the Wilcoxon rank sum test were manually inspected, and names were assigned based on gene enrichment per cluster. Differential expression analysis across clusters was performed using a multiple comparisons-adjusted Wilcoxon rank sum test. Pseudotime reconstruction was performed using Monocle3 (Cao et al. 2019). Pathway analysis was performed using the SCPA package using Gene Ontology Biological Process term lists (Bibby et al. 2022).

3 | Results

3.1 | Early Developmental Decrease in Neuronal Activity in the Olfactory System Increases Oligodendrocyte Differentiation

Unilateral naris occlusion (UNO), where one nostril is permanently occluded, is a well-established model of reduced neuronal activity in the olfactory system (Coppola 2012). UNO was induced at P0 to study the effect of reduced neuronal activity on oligodendrocyte development in the LOT at P5 (Figure 1A). To confirm successful occlusion, cFos expression was assessed in the mitral and tufted cell layer of the olfactory bulb (Figure 1B). Since mitral and tufted cells do not express NeuN but are stained by the pan-neuronal marker NISSL, we quantified cFos+ NISSL+ NeuN− active mitral/tufted cells (Figure 1C,D). NISSL+ NeuN− neurons in the mitral and tufted cell layer showed reduced cFos expression on the occluded side, confirming decreased neuronal activity following UNO. Notably, neuronal cell body and axon staining revealed no gross anatomical or axon changes in the olfactory bulb or LOT (data not shown).

Oligodendrocyte lineage cells in the occluded (ipsilateral) and non-occluded (contralateral) LOT were quantified using PDGFRα to visualize OPCs, BCAS1 for premyelinating oligodendrocytes, and PLP1 for maturing oligodendrocytes. Although decreased neuronal activity did not affect the number of OPCs, surprisingly, the occluded LOT exhibited an increase in BCAS1+ premyelinating cells and PLP1+ maturing cells compared to the non-occluded LOT (Figure 1E,F). These results indicate that decreased neuronal activity increased oligodendrocyte differentiation, supporting the idea that normal neuronal activity at this developmental stage acts to reduce OPC differentiation.

3.2 | Chemogenetic Reduction of Glutamatergic Neuronal Activity Increases Oligodendrocyte Differentiation, But Not Proliferation

To investigate if this apparent negative impact of neuronal activity on early OPC differentiation occurs elsewhere in the nervous system, we studied the developing somatosensory cortex and its axonal projections through the corpus callosum. In the somatosensory cortex, glutamatergic pyramidal neurons from layer II/III and V project to the same layers in the opposite hemisphere via the corpus callosum (Zhou et al. 2013; Wang et al. 2007). Importantly, during early postnatal development, there is extensive early axonal exuberance followed by dynamic circuit refinement (De León Reyes et al. 2020). In the corpus callosum, OPCs start to differentiate into premyelinating oligodendrocytes around P7 and robust myelination begins around P14 (Dawson et al. 2003). Thus, the first week of postnatal development provides a unique environment for studying how axonal development and activity influences early oligodendrogenesis prior to the onset of myelination in the cortex and corpus callosum.

We used chemogenetics to reduce glutamatergic neuronal activity in the somatosensory cortex from P2–P8. The AAV vector encoding inhibitory designer receptors exclusively activated by designer drugs (DREADDs), AAV-hSyn-DIO-hM4D(Gi)-mCherry (Gi-DREADD), was transduced into *Neurod6*$^{tm1(cre)Kan}$ (NexCre) (Goebbels et al. 2006) cortex at P0 and mice were treated with the designer drug, clozapine N-oxide (CNO) from P2–P8 to reduce depolarizing activity in somatosensory cortical neurons (Figure 2A). After injecting AAV-DREADD at P0, high mCherry expression was noted in neuronal soma in cortical L2/3, L4 and L5 of the somatosensory cortex, along with high mCherry expression in axons in the corpus callosum at P8 (Figure S1). A decrease in resting membrane potential (RMP) and an increase in rheobase in the presence of CNO (1 μM) was confirmed in mCh-expressing cortical neurons from NexCre+ mice by electrophysiology (Figure 2B). Additionally, decreased cFos+ neurons were noted in L4 and 5 somatosensory cortex, further demonstrating decreased neuronal activity in NexCre+ animals (Figure S1). OPCs (PDGFRα-positive) and premyelinating

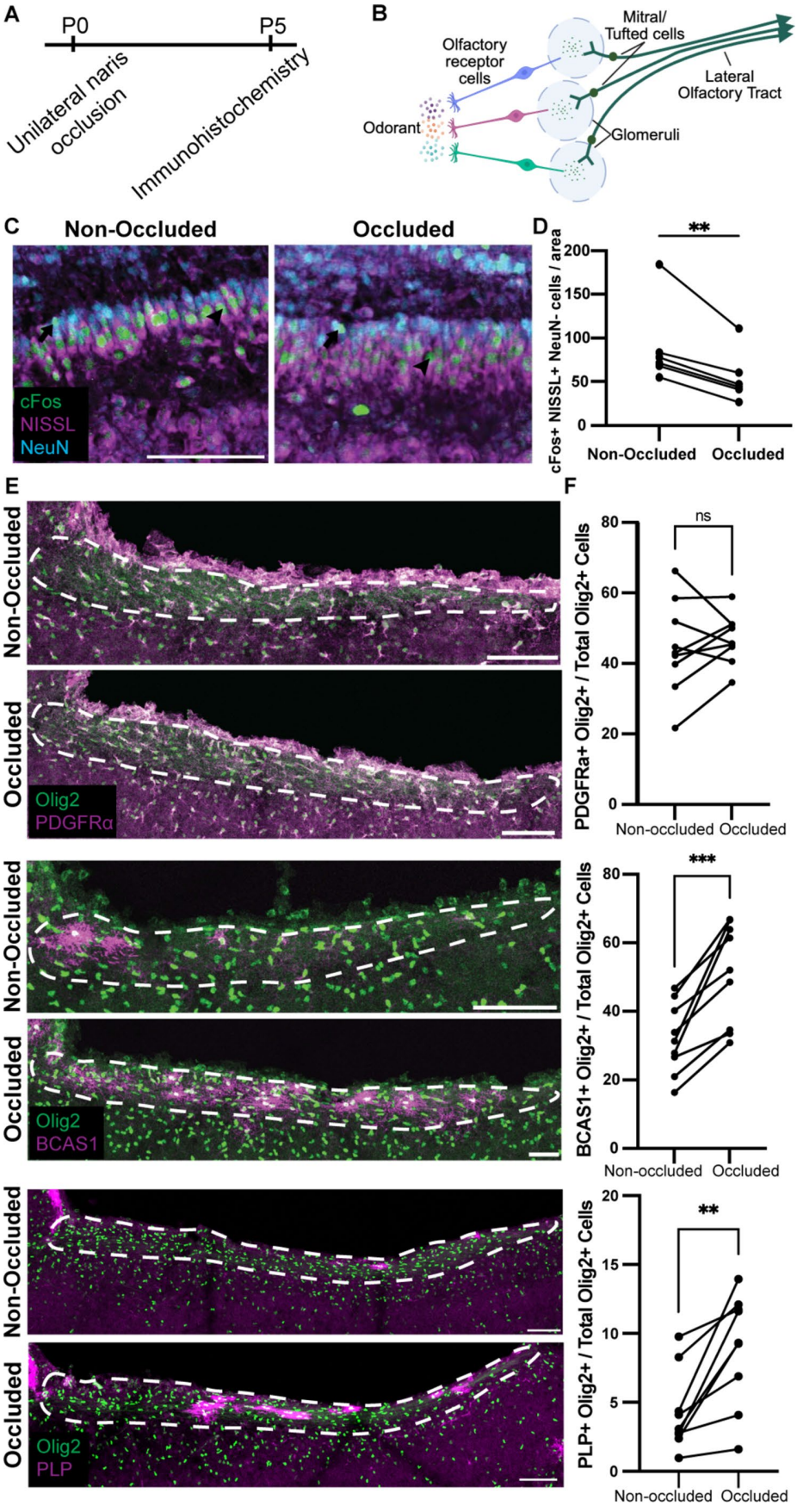

FIGURE 1 | Legend on next page.

FIGURE 1 | Unilateral naris occlusion causes increased differentiation of oligodendrocytes in the lateral olfactory tract. (A) Experimental timeline. P0 animals underwent UNO and were analyzed by immunohistochemistry at P5. (B) Schematic of olfactory system. (C) Validation of occlusion with cFos at P5. Images are from the tufted/mitral cell layer where cells that were negative for NeuN, positive for NISSL, and positive for cFos (arrowhead) were analyzed. Cells positive for NeuN (arrow) were not analyzed as mitral and tufted cells do not express NeuN. Scale bar is 100 μm. (D) Analysis of cFos+ mitral and tufted cells from occluded and non-occluded olfactory bulbs. (E) Immunostaining of oligodendrocyte lineage markers Olig2, PDGFRα, BCAS1 and PLP. Dotted outline represents LOT. (F) Quantification of PDGFRα, BCAS1 and PLP as a percentage of total Olig2 + cells in the LOT. Scale bar is 100 μm. Data from three sections each were averaged per animal. $n = 9$ mice. Paired Student's *t*-test. ns, not significant, $^{**}p < 0.01$, $^{***}p < 0.001$.

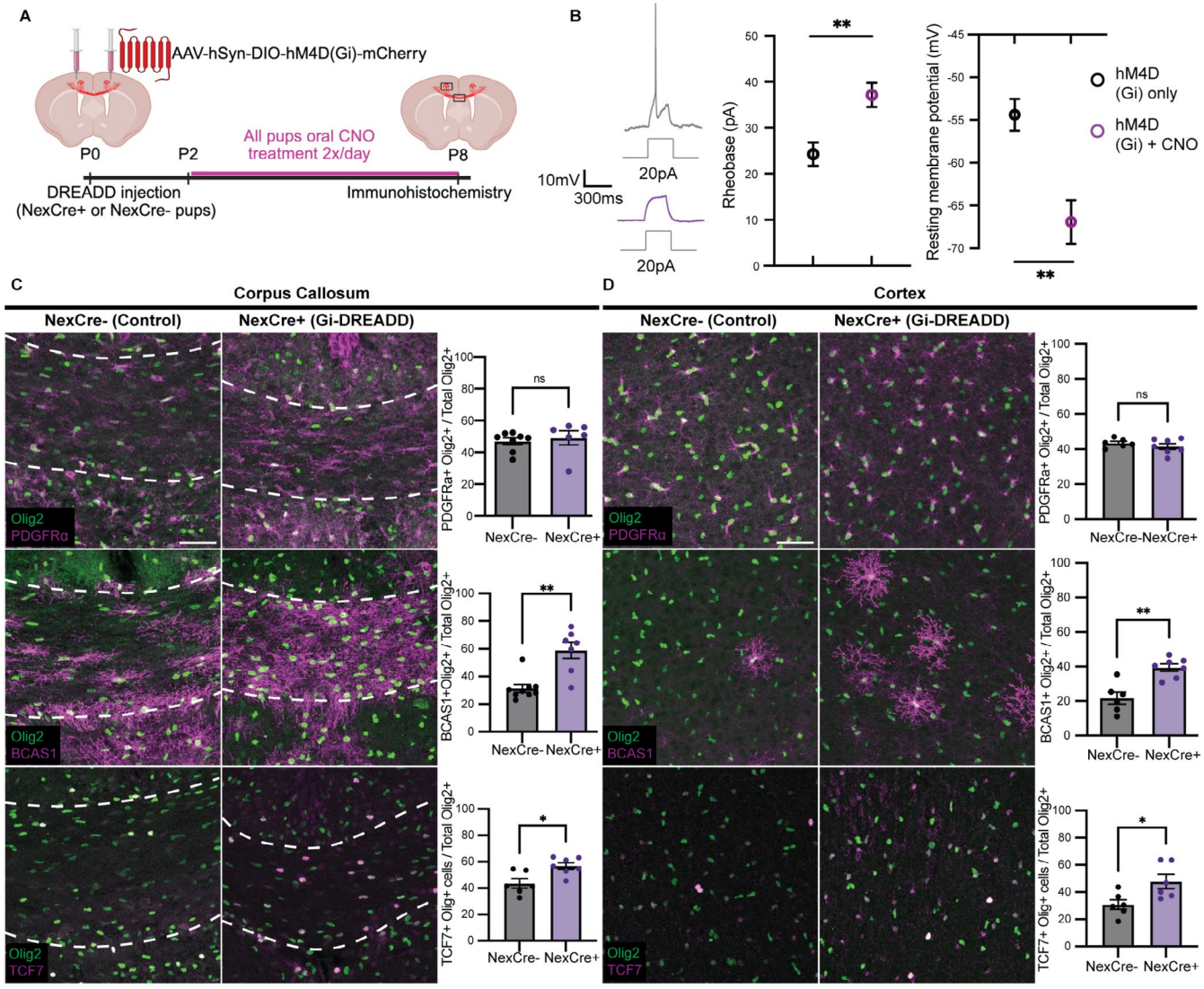

FIGURE 2 | Decreased neuronal activity drives OPC differentiation. (A) NexCre+ and NexCre− control litter mates were injected at P0 or P1 with AAV-hSyn-DIO-hM4D(Gi)-mCherry (Gi-DREADD), and orally administered CNO twice daily from P2–P8. Brains were imaged in L4 cortex and midline corpus callosum as indicated by the black boxes. (B) Acute slices were taken from NexCre+ P6 or P7 pups and whole-cell patch clamp recordings were performed from mCherry-expressing neurons. RMP and rheobase were recorded with and without CNO in the media. $n = 7$ neurons from two mice. (C) Representative images and quantification of the corpus callosum, and (D) L4 Somatosensory cortex show Olig2 along with PDGFRα (OPCs), BCAS1 (premyelinating) and TCF7 (premyelinating). Data from three sections each were averaged per animal. $n = 7$ NexCre− control mice and 8 NexCre+ mice. Scale bar is 50 μm. Student's *t*-test. ns, not significant $^{*}p < 0.05$, $^{**}p < 0.01$, $^{****}p < 0.0001$.

cells (BCAS1-positive and TCF7-positive) were quantified; consistent with the UNO results, no difference in OPC cell numbers was found in either the corpus callosum or the cortex. Notably, we found an increase in premyelinating cells in both the corpus callosum and cortex, showing increased differentiation of oligodendrocytes when neuronal activity was chronically reduced (Figure 2C,D). This suggests that, prior to the onset of myelination, neuronal activity negatively impacts

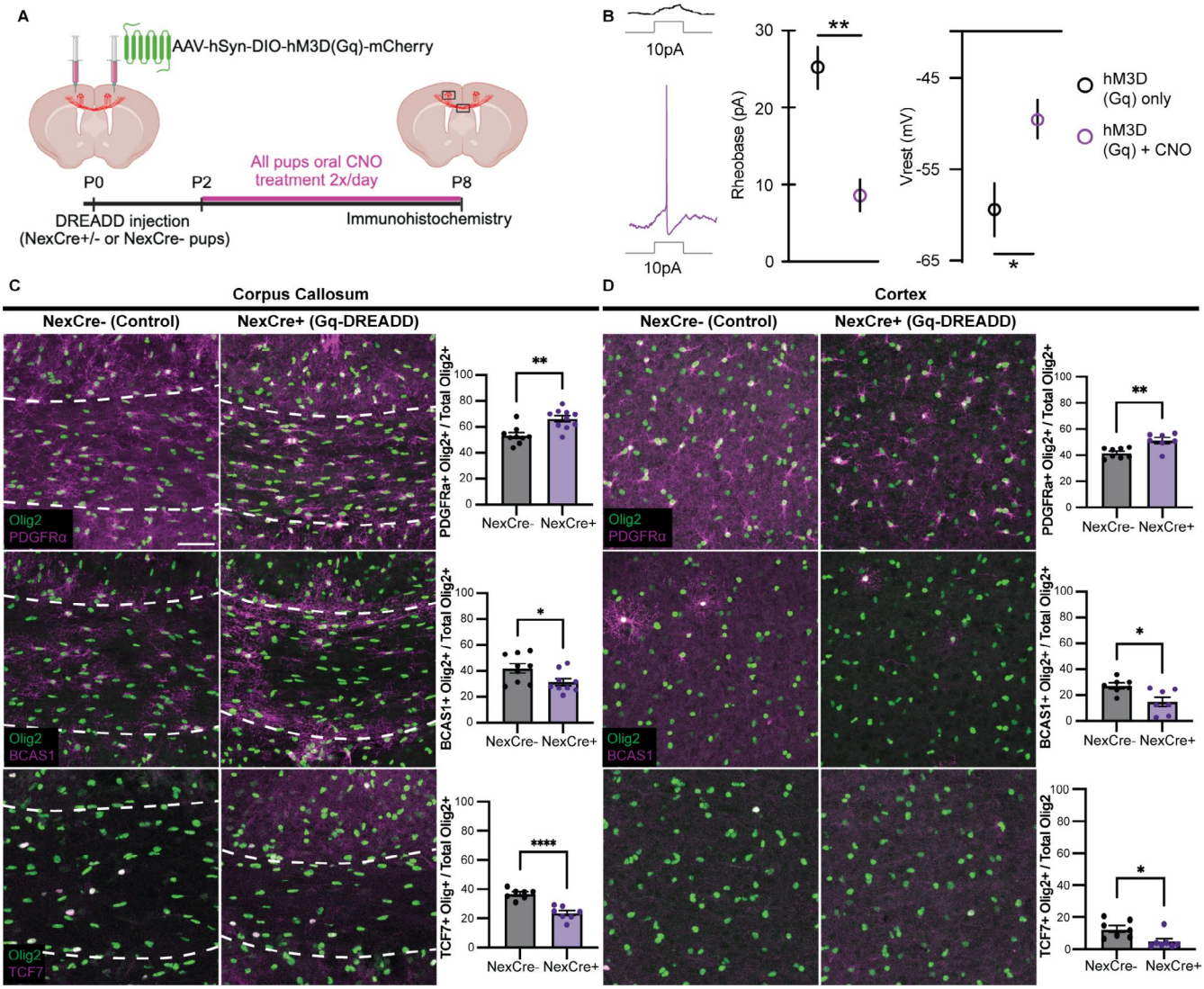

FIGURE 3 | Increased neuronal activity decreases oligodendrocyte differentiation. (A) Experimental design: NexCre+ and NexCre− control littermates were injected at P0 or P1 with pAAV-hSyn-DIO-hM3D(Gq)-mCherry, and orally administered CNO twice daily from P2–P8. (B) Acute slices were taken from NexCre+ pups and whole-cell patch clamp recordings were performed from mCherry-expressing neurons. Representative traces show voltage response to 10 pA injection with and without CNO. Rheobase and resting membrane potential (Vrest) were recorded with and without CNO in the media. Data is from 7 neurons from 2 pups P7 and P8. (C) Representative images and quantification of the corpus callosum, and (D) Somatosensory cortex show Olig2 along with PDGFRα (OPCs), BCAS1 (premyelinating) and TCF7 (premyelinating). Scale bar is 50 μm. Data from three sections each were averaged per animal. $n = 7–11$ NexCre− control mice and 7–12 NexCre+ mice. Student's t-test. ns, not significant $^{*}p < 0.05$, $^{**}p < 0.01$, $^{****}p < 0.0001$.

oligodendrocyte differentiation. Surprisingly, no change in OPC proliferation was seen (Figure S2), suggesting that at these early time points, neuronal activity does not influence OPC proliferation. Together, these data show decreased neuronal activity at this early age increases oligodendrocyte differentiation.

3.3 | Increased Excitation of Glutamatergic Neurons Decreases Oligodendrocyte Differentiation, But Not Proliferation

To directly confirm our hypothesis that neuronal activity negatively regulates oligodendrocyte differentiation in early postnatal development, we transduced the excitatory DREADD, AAV-hSyn-DIO-hM3D(Gq)-mCherry (Gq-DREADD), into Nex-Cre cortical neurons at P0 and activated it with CNO from P2–P8 (Figure 3A). Slice electrophysiology confirmed that Gq-DREADD-expressing neurons exhibited an increased RMP and decreased rheobase upon bath application of CNO (Figure 3B). Additionally, there was an increase in cFos+ neurons in L4 and 5 somatosensory cortex of NexCre+ animals compared to NexCre− animals, further confirming increased neuronal activity (Figure S1).

OPCs and premyelinating oligodendrocytes were again quantified. Excitingly, increased neuronal activity reduced the number of BCAS1+ and TCF7+ premyelinating cells in the cortex

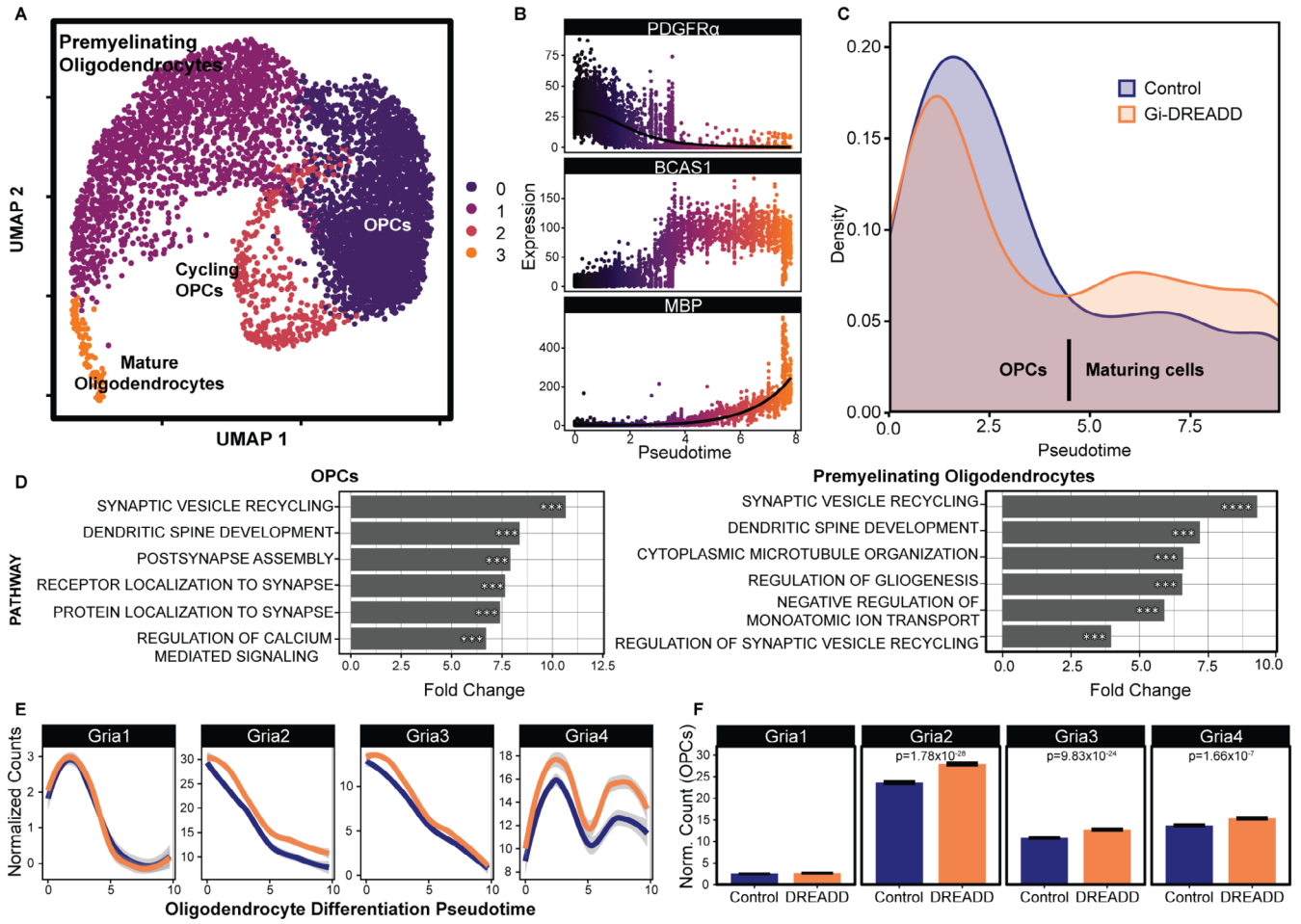

FIGURE 4 | Decreased neuronal activity changes oligodendrocyte lineage gene expression and causes upregulation of AMPAR genes. NexCre− (control, blue) and NexCre+ (DREADD, orange) were injected at P0 or P1 with AAV-hSyn-DIO-hM4D(Gi)-mCherry, and orally administered CNO twice daily from P2–P8. Brains from 3 animals each were pooled and homogenized. Oligodendrocytes were separated for sequencing by magnetic beads conjugated to PDGFRα and O4. scRNAseq analysis reveal transcriptional changes in oligodendrocyte lineage cells. (A) UMAP embedding showing oligodendrocyte lineage cells from DREADD ($n = 3$ mice pooled) and control ($n = 2$ mice pooled) (peach cluster: Cycling OPCs, purple cluster: OPCs, maroon cluster: Premyelinating oligodendrocytes, orange cluster: Mature oligodendrocytes). Refer to Figure S3 for more detail (QC). (B) Oligodendrocyte lineage markers across a pseudotime cell state trajectory (Pdgfrα+ OPCs pseudotime < 4, Bcas1+ premyelinating cells pseudotime > 4 and < 6, Mbp+ mature cells pseudotime > 6). (C) Kernel density estimate of DREADD treated and control cells across pseudotime showing altered distribution of cell states. (D) Differential pathway analysis for OPC cluster (left) and premyelinating cell clusters (right) revealed synapse development and maintenance pathways. Bonferroni adjusted p values $^{***}p < 1 \times 10{-}20$, $p < 6 \times 10{-}20$. Wilcoxon rank sum test. (E) SCTransform normalized counts of GluR genes across differentiation pseudotime (control: Blue, DREADD: Orange). (F) AMPAR gene expression in OPCs. SCTransform normalized counts. Bonferroni adjusted p values. Wilcoxon rank sum test. Extended data Table S1 for details.

and corpus callosum (Figure 3C,D). These data further confirm our hypothesis that neuronal activity is a negative regulator of oligodendrocyte maturation in early development. Surprisingly, PDGFRα+ OPCs in both the corpus callosum and cortex were increased in response to increased neuronal activity. Similar to the Gi-DREADD experiment, there was no change in OPC proliferation (Figure S2); thus, the increase in OPCs could be due to an accumulation of OPCs that are inhibited from differentiating. This further suggests that neuronal activity does not regulate proliferation at these early developmental time points; rather, it independently affects differentiation, supporting our hypothesis that excitatory neuronal activity reduces oligodendrocyte maturation in early brain development prior to the onset of myelination.

3.4 | Oligodendroglial Glutamate Receptor Expression Is Altered in Response to Reduced Neuronal Activity

To investigate the impact of decreased neuronal activity on early oligodendrocyte gene expression, oligodendrocyte lineage cells from Gi-DREADD-transduced, CNO-treated mice (as in Figure 2A) were isolated using magnetic bead separation and analyzed by single-cell RNA sequencing (see methods). Unsupervised clustering analysis showed successful isolation of OPCs and oligodendrocytes along a continuum of differentiation states (Figure 4A). To understand changes along this continuum, a pseudotime analysis was performed, which defined a path of state transitions between OPCs and oligodendrocytes

(Figure 4B). The overall distribution of cells in the NexCre+ group was shifted towards more differentiated states compared to the control group (Figure 4C), which is consistent with our in vivo data showing increased oligodendrocyte maturation in response to reduced neuronal activity (Figure 2). Importantly, pseudotime analysis allows for comparison of RNA changes in cells of like states, studying OPC differentiation between NexCre− control (cells exposed to normal neuronal activity) and NexCre+ (cells exposed to decreased neuronal activity). Thus, cells of equivalent differentiation states are compared in both conditions.

Pathway analysis revealed a variety of upregulated pathways in OPCs and premyelinating oligodendrocytes, including pathways related to postsynapse remodeling (Figure 4D). These data suggest that reduced glutamatergic neuronal activity regulates neuron-oligodendrocyte synapses in both OPCs and premyelinating cells. A variety of differentially expressed genes in response to decreased neuronal activity were identified, but interestingly, the expression of several glutamate receptor genes was significantly increased in the Gi-DREADD condition (Figure 4E,F), again suggesting the importance of direct communication between neurons and oligodendrocytes. Notably, the AMPA receptor gene, *Gria2*, was upregulated across the entire oligodendrocyte lineage, and *Gria3* and *Gria4* were upregulated in OPCs (Figure 4E,F). These data show significant expression of AMPA receptor genes in oligodendrocytes at these early developmental time points, and that their expression changes in response to neuronal activity, with upregulation when neuronal activity is reduced. This suggests an important role for oligodendroglial AMPA receptors in responding to neuronal activity to regulate oligodendrocyte maturation in early development.

3.5 | AMPAR Stimulation Rescues Inhibitory Effects of Neuronal Activity on Oligodendrocyte Differentiation

To directly test whether oligodendroglial AMPA receptors mediate the activity-dependent regulation of oligodendrocyte maturation, we next turned to an ex vivo cortical slice culture system that allowed pharmacological manipulation of neuronal activity and AMPARs. We first established a timeline for oligodendrocyte development ex vivo in slices from P4 mice and found peak differentiation between 6 and 8 days in vitro (DIV) (Figure 5A,B). To confirm that neuronal activity has a comparable negative regulatory effect on oligodendrocyte differentiation ex vivo to that in vivo (Figures 2 and 3), the Na^+ channel inhibitor, tetrodotoxin (TTX), was applied for 48 h to silence all electrical activity. This treatment increased the proportion of cells positive for the mature oligodendrocyte marker, PLP (Figure 5C). Interestingly, the proportion of PDGFRα+ OPCs was decreased and BCAS1+ cells were unchanged following treatment, suggesting a shift to a more mature cell type. Furthermore, pharmacological inhibition of AMPARs with NBQX for 48 h similarly promoted oligodendrocyte differentiation, indicating a critical role for AMPAR signaling in this process (Figure 5C).

To determine whether AMPAR stimulation can rescue the oligodendrocyte differentiation effect of inhibited neuronal activity, slices were treated with AMPA at the same time as TTX to silence neuronal activity while simultaneously stimulating AMPARs (AMPA). Silenced neuronal activity combined with AMPAR stimulation partially rescued the differentiation effect, as the proportion of mature, PLP+ oligodendrocytes returned to control levels (Figure 5C). This only partially rescued the decrease in PDGFRα+ OPCs. Unexpectedly, this also caused a dramatic increase in BCAS1+ premyelinating cells (Figure 5C). These data suggest that neuronal activity acts through AMPARs to regulate the late steps of oligodendrocyte differentiation to mature oligodendrocytes, but not the initiation of OPC differentiation to premyelinating cells.

Finally, to determine whether AMPAR stimulation can rescue the effect of DREADD-decreased neuronal activity, Gi-DREADD was used to chemogenetically reduce neuronal activity in glutamatergic projection neurons in cortical slice culture, after confirming that CNO treatment alone did not affect oligodendrocyte differentiation (Figure S4). As in vivo, Gi-DREADD activation with CNO for 48 h increased oligodendrocyte differentiation, shown by an increase in PLP+ mature cells (Figure S5). Again, no change in the proportion of OPCs or premyelinating cells was observed, suggesting that OPCs can differentiate to maturity in 48 h (Figure S5). To address the contribution of AMPARs to this phenotype, Gi-DREADD-expressing explants were exposed to CNO + AMPA to reduce neuronal activity while simultaneously stimulating AMPARs. Reduced neuronal activity combined with AMPAR stimulation partially rescued the differentiation effect, as the proportion of mature, PLP+ oligodendrocytes returned to control levels (Figure 5C). This also caused a decrease in PDGFRα+ OPCs and a dramatic increase in BCAS1+ premyelinating cells, similar to TTX + AMPA treatment (Figures 5C and S5). Combined, these data suggest that neuronal activity acts through AMPARs to regulate the late steps of oligodendrocyte differentiation to mature oligodendrocytes, but not the initiation of OPC differentiation to premyelinating cells.

4 | Discussion

Here we address how neuronal activity influences oligodendrogenesis in early mouse development and find a novel role for neuronal activity in OPC differentiation: prior to the onset of developmental myelination, neuronal activity reduces oligodendrocyte differentiation, which is mediated in part by oligodendroglial AMPA receptors. A few studies have investigated this developmental question, also finding that reduced neuronal activity in early development increases oligodendrogenesis in the barrel cortex and the retinogeniculate pathway (Mangin et al. 2012; Etxeberria et al. 2016). With a similar sensory deprivation approach using UNO, we show that decreased activity of mitral and tufted cells in the olfactory bulb projecting through the LOT (subsequently a highly myelinated white matter tract) caused an increase in OPC differentiation in the LOT (Figure 1). This contrasts with studies in the adult olfactory system including from our group, using UNO to address the regulation of myelination (Collins et al. 2018; George et al. 2022), which found decreased myelination in response to reduced neuronal activity. Our current findings are consistent with the Mangin et al. (2012) and Etxeberria et al. (2016) studies on the development of the barrel cortex and the retinogeniculate pathway, pointing to unique communication between neurons and oligodendrocytes in early development prior to the onset of myelination.

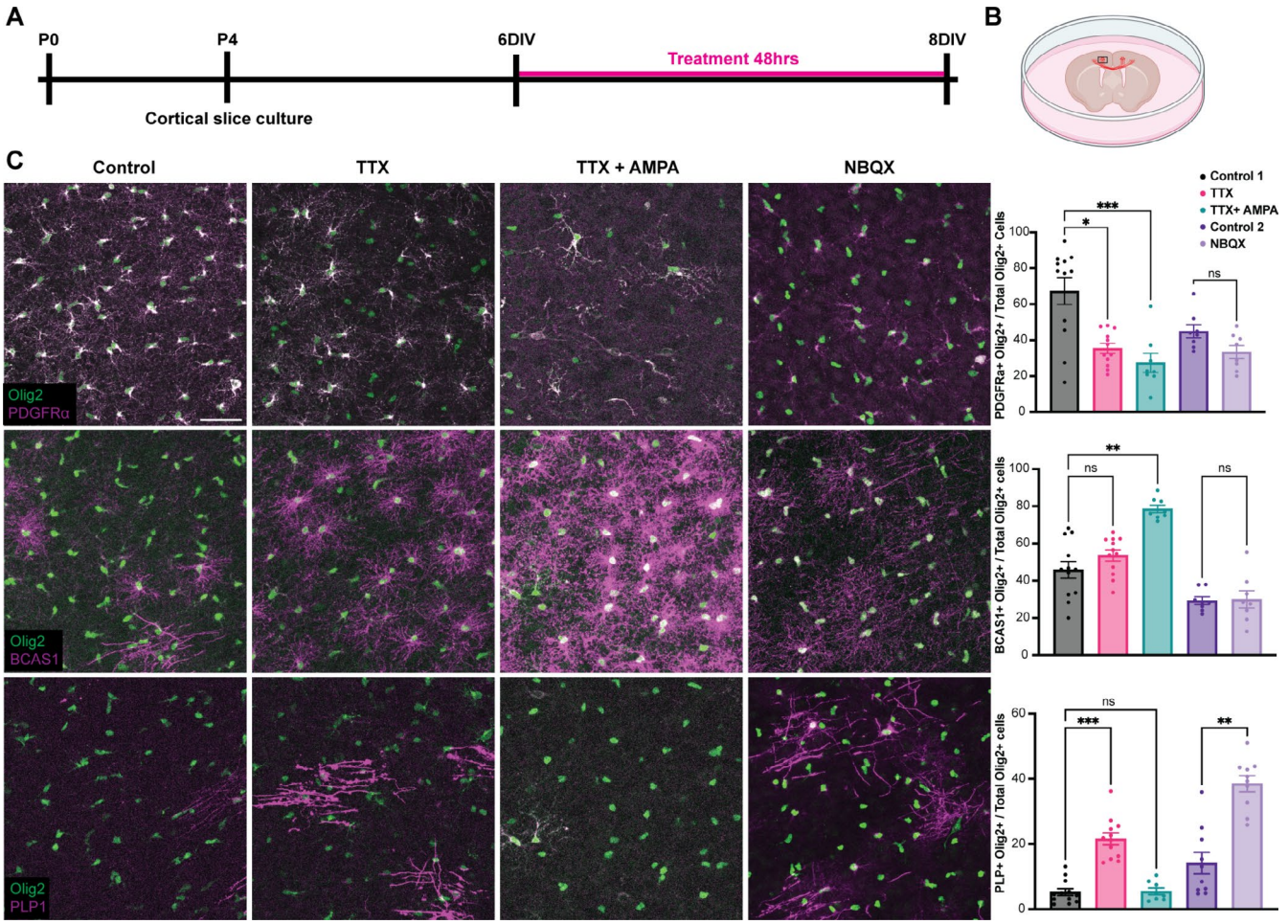

FIGURE 5 | Silenced electrical activity increases oligodendrocyte differentiation and AMPAR stimulation regulates this effect. (A) Schematic of experimental design. WT pups were taken at P4, and 300 μm thick slices of cortex were plated on a membrane. At 6 and 7DIV, the indicated drug was bath applied to slices, and slices were fixed and stained 48 h later at 8DIV. (B) Schematic of slice culture. Black square represents the area where images were taken. (C) Images and quantification of PDGFRα (OPCs), BCAS1 (pre-myelinating oligodendrocytes) and PLP (maturing oligodendrocytes) in each experimental condition. Control 1 is media alone and was performed at the same time as TTX and TTX + AMPA. Control 2 is media + CNO and was performed at the same time as NBQX (see Figure S4 for CNO controls). Statistics were done separately as indicated. Scale bar is 50 μm. $n = 8$–12 mice. One-way ANOVA Kruskal-Wallis test with multiple comparisons to appropriate corresponding control group. ns, not significant; $^{*}p < 0.05$; $^{**}p < 0.01$; $^{***}p < 0.001$.

With a goal of directly addressing glutamatergic neuronal activity specifically, we used chemogenetics in NexCre mice. Decreased neuronal activity following Gi-DREADD activation resulted in increased OPC differentiation, similar to our UNO model (Figure 2). Electrical and proliferative properties of OPCs at early ages (P6) are indistinguishable across brain regions (Pivoňková et al. 2024; Spitzer et al. 2019), which is consistent with our data showing comparable OPC responses to altered neuronal activity in both gray matter (cortex) and future white matter (corpus callosum) in these early ages. Further studies using Gq-DREADDs expressed in glutamatergic projection neurons increased neuronal activity, which in turn *reduced* OPC differentiation into premyelinating oligodendrocyte states (Figure 3). Again, no differences were noted in cortex relative to corpus callosum OPC responses (Figures 2 and 3), that is, increased neuronal activity decreased differentiation in both regions. Interestingly, no differences in OPC proliferation occurred in response to increased neuronal activity, as seen in adult models (Barres and Raff 1993; Gibson et al. 2014; Mitew et al. 2018), suggesting a developmental context-dependent role for neuronal activity in OPC development. Together, these data show that, contrary to adult models, neuronal activity reduces oligodendrocyte differentiation in early development.

Projection neurons from the cortex cross the midline as early as embryonic day 15, but these neurons are dynamically refined and stabilized during early postnatal development (Rash and Richards 2001; De León Reyes et al. 2020). In early development, young neurons are highly exuberant (Innocenti and Price 2005), that is, over-abundant and highly active, but they are not yet myelinated. Therefore, in early development, oligodendrocytes may respond to these activity cues differently than in later development and adulthood when increased activity promotes myelination. Together, these findings show that across physiological (UNO) and experimentally manipulated contexts (DREADDs), and in multiple brain regions (LOT, L4 and 5 somatosensory cortex, and corpus callosum), early developmental neuronal activity normally reduces oligodendrocyte differentiation and that block can be reversed by reducing neuronal activity (Figures 1–3).

The increases in OPC differentiation were driven by decreased neuronal activity in our models, but we wanted to address the underlying transcriptional changes occurring in early oligodendrocytes in response to reduced neuronal activity. Pathway analysis of gene expression changes in response to decreased neuronal activity unsurprisingly identified increased regulation of gliogenesis, but also identified several interesting pathways related to synapse development and organization. Importantly, we found differential regulation of glutamate receptors: AMPAR subunit gene expression in oligodendrocytes increased in response to reduced neuronal activity, which is comparable to the neuronal response to decreased neuronal activity (O'Brien et al. 1998). Given that Gria2 and Gria3 RNAs are highly expressed in OPCs and committed oligodendrocyte progenitors and then normally drop with differentiation (Marques et al. 2016), this upregulation would be unexpected if this were simply a response to increased differentiation. This is likely a compensatory response to reduced glutamatergic input to these OPCs upon reduction in neuronal activity, and it highlights the critical role of neurotransmitter signaling in oligodendrocyte development. These analyses also introduce the question of how AMPARs are involved in oligodendrocyte maturation.

OPCs form direct synapses with glutamatergic neurons, and they respond electrically to glutamate through AMPAR stimulation as early as P7 and throughout the lifespan (Bergles et al. 2000). Numerous studies have investigated the potential role of glutamatergic signaling to oligodendrocytes across development and adulthood (Perez-Gianmarco et al. 2023; Jansson and Åkerman 2014), including a previous study from our group showing that the GluA2 subunit of AMPARs regulates OPC migration, and other studies addressing their role in oligodendrocyte survival (Harlow et al. 2015; Kougioumtzidou et al. 2017). There is less consensus on the role of AMPARs in oligodendrogenesis. Consistent with the concept that neuronal activity promotes oligodendrogenesis, studies in juvenile and adult mice have shown that AMPAR stimulation also promotes oligodendrogenesis in vivo (Chen et al. 2018; Kougioumtzidou et al. 2017). These studies focused on the role of oligodendroglial AMPARs in juvenile and adult mice, again after the onset of developmental myelination. Conversely, other studies have used in vitro and ex vivo models to show that decreased neuronal activity or AMPAR inhibition causes increased OPC proliferation and increased oligodendrocyte differentiation (Gallo et al. 1996; Yuan et al. 1998; Fannon et al. 2015). It should be noted that these in vitro and ex vivo studies more closely recapitulate an early developmental environment as explants and primary cells are taken from early postnatal mice. Nevertheless, these seemingly conflicting results support the concept of a developmental shift in AMPAR-mediated signaling, whereby prior to myelination, glutamatergic activity via AMPARs suppresses oligodendrocyte differentiation, but following the onset of myelination, AMPAR activation facilitates oligodendrogenesis to meet the demand for new myelin. Thus, AMPAR signaling regulates oligodendrocyte development in a stage- and context-dependent manner.

Our ex vivo system allows for greater experimental manipulations to study the effects of neuronal activity and AMPARs. Pharmacological inhibition (TTX) and chemogenetic reduction (Gi-DREADD) of neuronal activity increased oligodendrocyte differentiation, recapitulating our in vivo results (Figures 2, 5 and S5), and blocking AMPARs with NBQX also increased oligodendrocyte differentiation, confirming previous studies (Gallo et al. 1996; Fannon et al. 2015). Excitingly, blocked or reduced neuronal activity with simultaneous AMPAR stimulation rescued the increased differentiation effect of altered neuronal activity that pushed oligodendrocytes to the mature PLP+ state (Figures 5 and S5). These findings suggest that in early development, glutamate released from neurons signals through OPC AMPARs to reduce oligodendrocyte differentiation. When this block is released by reducing neuronal activity or by blocking AMPARs, oligodendrocytes respond by differentiating. Caveats to this interpretation include that neurons could signal through different glutamate receptors on oligodendrocytes, or through other cells, such as astrocytes, and not act directly on oligodendrocytes. Further, Gi-DREADDs only reduce activity from a subset of neurons. However, TTX inhibits all action potentials, such that adding AMPA cannot restore normal neuronal activity. This approach provides clear evidence that oligodendrocyte AMPAR stimulation regulates oligodendrocyte differentiation.

An exciting result of this experiment is that AMPAR stimulation when neuronal activity was blocked only partially rescued the differentiation phenotype. In this context, the proportion of OPCs was reduced and, unexpectedly, the proportion of premyelinating cells was greatly increased, and the proportion of PLP+ mature cells returned to control levels. This suggests that neuronal activity influences oligodendrocytes by multiple mechanisms, with AMPAR stimulation regulating the later maturation steps, whereas neuronal activity independent of AMPAR signaling acts to regulate the early phase of OPC differentiation. OPC differentiation to premyelinating cells is still increased with neuronal activity reduction even in the presence of AMPA, but the cells are held at the premyelinating cell stage. These data support the hypothesis that oligodendroglial AMPARs play a key role in communication between excitatory neurons and developing oligodendrocytes, but they highlight the multiple stages at which neuronal activity regulates oligodendrocyte differentiation. Overall, the findings in this study further highlight the context dependence of the interplay of neuronal activity, AMPAR stimulation and oligodendrocyte differentiation. Future studies should focus on the downstream mechanisms of AMPAR signaling in oligodendrocytes.

Author Contributions

T.E.A. performed all in vivo and ex vivo experiments. L.E.G.W. and W.C.O. performed electrophysiology experiments. G.P. and T.E.A. performed clustering and pseudotime analysis. T.E.A. and W.B.M. designed experiments. T.E.A., W.B.M., and W.C.O. wrote the manuscript. W.B.M. and W.C.O. supervised the project.

Acknowledgments

Wendy Macklin and Won Chan Oh disclose support for this research from R21NS135041, Won Chan Oh discloses support from the University of Colorado Ludeman Family Center and NIH R01MH124778, Tessa Allen discloses support from NIH fellowship F31NS139593, Graham Peet discloses support from F31NS141369, Luis Gomez-Wulshner discloses support from F31DA060091. This work would not have been possible without the support of the Genomics Core Shared Resource at University of Colorado, Anschutz and their funding from NIH

P30CA046934 funded genomics shared resource (RRID: SCR 021984). The Nex-Cre mice were obtained through the Max Planck Institute of Experimental Medicine, Göttingen, Germany. Finally, we acknowledge Dr. Kenneth Jones for important discussions.

Funding

This work was supported by the National Institute of Neurological Disorders and Stroke, R21NS135041, F31NS139593, F31NS141369 and the national institute of health P30CA046934 funded genomics shared resource (RRID: SCR_021984).

Conflicts of Interest

The authors declare no conflicts of interest.

Data Availability Statement

The data that support the findings of this study will be openly available in Gene Expression Omnibus upon publication.

References

Barres, B. A., and M. C. Raff. 1993. "Proliferation of Oligodendrocyte Precursor Cells Depends on Electrical Activity in Axons." *Nature* 361: 258–260.

Bergles, D. E., J. D. Roberts, P. Somogyi, and C. E. Jahr. 2000. "Glutamatergic Synapses on Oligodendrocyte Precursor Cells in the Hippocampus." *Nature* 405: 187–191.

Bibby, J. A., D. Agarwal, T. Freiwald, et al. 2022. "Systematic Single-Cell Pathway Analysis to Characterize Early T Cell Activation." *Cell Reports* 41: 111697.

Cao, J., M. Spielmann, X. Qiu, et al. 2019. "The Single-Cell Transcriptional Landscape of Mammalian Organogenesis." *Nature* 566: 496–502.

Chen, T.-J., B. Kula, B. Nagy, et al. 2018. "In Vivo Regulation of Oligodendrocyte Precursor Cell Proliferation and Differentiation by the AMPA-Receptor Subunit GluA2." *Cell Reports* 25: 852–861.e7.

Collins, L. N., D. L. Hill, and P. C. Brunjes. 2018. "Myelination of the Developing Lateral Olfactory Tract and Anterior Commissure." *Journal of Comparative Neurology* 526: 1843–1858.

Coppola, D. M. 2012. "Studies of Olfactory System Neural Plasticity: The Contribution of the Unilateral Naris Occlusion Technique." *Neural Plasticity* 2012: 351752.

Cristobal, C. D., and H. K. Lee. 2022. "Development of Myelinating Glia: An Overview." *Glia* 70: 2237–2259.

Dawson, M. R. L., A. Polito, J. M. Levine, and R. Reynolds. 2003. "NG2-Expressing Glial Progenitor Cells: An Abundant and Widespread Population of Cycling Cells in the Adult Rat CNS." *Molecular and Cellular Neurosciences* 24: 476–488.

De Biase, L. M., A. Nishiyama, and D. E. Bergles. 2010. "Excitability and Synaptic Communication Within the Oligodendrocyte Lineage." *Journal of Neuroscience: The Official Journal of the Society for Neuroscience* 30: 3600–3611.

De León Reyes, N. S., L. Bragg-Gonzalo, and M. Nieto. 2020. "Development and Plasticity of the Corpus Callosum." *Development* 147: dev189738.

Etxeberria, A., K. C. Hokanson, D. Q. Dao, et al. 2016. "Dynamic Modulation of Myelination in Response to Visual Stimuli Alters Optic Nerve Conduction Velocity." *Journal of Neuroscience: The Official Journal of the Society for Neuroscience* 36: 6937–6948.

Fannon, J., W. Tarmier, and D. Fulton. 2015. "Neuronal Activity and AMPA-Type Glutamate Receptor Activation Regulates the Morphological Development of Oligodendrocyte Precursor Cells." *Glia* 63: 1021–1035.

Foran, D., and A. Peterson. 1992. "Myelin Acquisition in the Central Nervous System of the Mouse Revealed by an MBP-Lac Z Transgene." *Journal of Neuroscience* 12: 4890–4897.

Foster, A. Y., H. Bujalka, and B. Emery. 2019. "Axoglial Interactions in Myelin Plasticity: Evaluating the Relationship Between Neuronal Activity and Oligodendrocyte Dynamics." *Glia* 67: 2038–2049.

Gallo, V., J. M. Zhou, C. J. McBain, et al. 1996. "Oligodendrocyte Progenitor Cell Proliferation and Lineage Progression Are Regulated by Glutamate Receptor-Mediated K+ Channel Block." *Journal of Neuroscience: The Official Journal of the Society for Neuroscience* 16: 2659–2670.

George, N. M., A. Gentile Polese, L. Merle, W. B. Macklin, and D. Restrepo. 2022. "Excitable Axonal Domains Adapt to Sensory Deprivation in the Olfactory System." *Journal of Neuroscience: The Official Journal of the Society for Neuroscience* 42: 1491–1509.

Gibson, E. M., D. Purger, C. W. Mount, et al. 2014. "Neuronal Activity Promotes Oligodendrogenesis and Adaptive Myelination in the Mammalian Brain." *Science* 344: 1252304.

Goebbels, S., I. Bormuth, U. Bode, et al. 2006. "Genetic Targeting of Principal Neurons in Neocortex and Hippocampus of NEX-Cre Mice." *Genesis* 44: 611–621.

Gudz, T. I., H. Komuro, and W. B. Macklin. 2006. "Glutamate Stimulates Oligodendrocyte Progenitor Migration Mediated via an αv Integrin/Myelin Proteolipid Protein Complex." *Journal of Neuroscience* 26: 2458–2466.

Hao, Y., T. Stuart, M. H. Kowalski, et al. 2024. "Dictionary Learning for Integrative, Multimodal and Scalable Single-Cell Analysis." *Nature Biotechnology* 42: 293–304.

Harlow, D. E., K. E. Saul, H. Komuro, and W. B. Macklin. 2015. "Myelin Proteolipid Protein Complexes With αv Integrin and AMPA Receptors In Vivo and Regulates AMPA-Dependent Oligodendrocyte Progenitor Cell Migration Through the Modulation of Cell-Surface GluR2 Expression." *Journal of Neuroscience: The Official Journal of the Society for Neuroscience* 35: 12018–12032.

Innocenti, G. M., and D. J. Price. 2005. "Exuberance in the Development of Cortical Networks." *Nature Reviews. Neuroscience* 6: 955–965.

Jansson, L. C., and K. E. Åkerman. 2014. "The Role of Glutamate and Its Receptors in the Proliferation, Migration, Differentiation and Survival of Neural Progenitor Cells." *Journal of Neural Transmission* 1996, no. 121: 819–836.

Khandker, L., M. A. Jeffries, Y. J. Chang, et al. 2022. "Cholesterol Biosynthesis Defines Oligodendrocyte Precursor Heterogeneity Between Brain and Spinal Cord." *Cell Reports* 38: 110423.

Kougioumtzidou, E., T. Shimizu, N. B. Hamilton, et al. 2017. "Signalling Through AMPA Receptors on Oligodendrocyte Precursors Promotes Myelination by Enhancing Oligodendrocyte Survival." *eLife* 6: e28080.

Logan, D. W., L. J. Brunet, W. R. Webb, et al. 2012. "Learned Recognition of Maternal Signature Odors Mediates the First Suckling Episode in Mice." *Current Biology* 22: 1998–2007.

Mangin, J.-M., P. Li, J. Scafidi, and V. Gallo. 2012. "Experience-Dependent Regulation of NG2 Progenitors in the Developing Barrel Cortex." *Nature Neuroscience* 15: 1192–1194.

Marques, S., A. Zeisel, S. Codeluppi, et al. 2016. "Oligodendrocyte Heterogeneity in the Mouse Juvenile and Adult Central Nervous System." *Science* 352: 1326–1329.

McDonald, J. W., S. P. Althomsons, K. L. Hyrc, D. W. Choi, and M. P. Goldberg. 1998. "Oligodendrocytes From Forebrain Are Highly

Vulnerable to AMPA/Kainate Receptor-Mediated Excitotoxicity." *Nature Medicine* 4: 291–297.

Mitew, S., I. Gobius, L. R. Fenlon, et al. 2018. "Pharmacogenetic Stimulation of Neuronal Activity Increases Myelination in an Axon-Specific Manner." *Nature Communications* 9: 306.

O'Brien, R. J., S. Kamboj, M. D. Ehlers, et al. 1998. "Activity-Dependent Modulation of Synaptic AMPA Receptor Accumulation." *Neuron* 21: 1067–1078.

Ogelman, R., L. E. Gomez Wulschner, V. M. Hoelscher, et al. 2024. "Serotonin Modulates Excitatory Synapse Maturation in the Developing Prefrontal Cortex." *Nature Communications* 15: 1368.

Oh, W. C., S. Lutzu, P. E. Castillo, et al. 2016. "Novo Synaptogenesis Induced by GABA in the Developing Mouse Cortex." *Science* 353: 1037–1040.

Oh, W. C., G. Rodríguez, D. Asede, et al. 2021. "Dysregulation of the Mesoprefrontal Dopamine Circuit Mediates an Early-Life Stress-Induced Synaptic Imbalance in the Prefrontal Cortex." *Cell Reports* 35: 109074.

Pati, S., K. Saba, S. S. Salvi, et al. 2020. "Chronic Postnatal Chemogenetic Activation of Forebrain Excitatory Neurons Evokes Persistent Changes in Mood Behavior." *eLife* 9: e56171.

Perez-Gianmarco, L., B. Kurt, and M. Kukley. 2023. "Technical Approaches and Challenges to Study AMPA Receptors in Oligodendrocyte Lineage Cells: Past, Present, and Future." *Glia* 71: 819–847.

Piller, M., I. L. Werkman, E. A. Brown, A. J. Latimer, and S. Kucenas. 2021. "Glutamate Signaling via the AMPAR Subunit GluR4 Regulates Oligodendrocyte Progenitor Cell Migration in the Developing Spinal Cord." *Journal of Neuroscience: The Official Journal of the Society for Neuroscience* 41: 5353–5371.

Pivoňková, H., S. Sitnikov, Y. Kamen, et al. 2024. "Heterogeneity in Oligodendrocyte Precursor Cell Proliferation Is Dynamic and Driven by Passive Bioelectrical Properties." *Cell Reports* 43: 114873.

R Core Team. 2021. R: A Language and Environment for Statistical Computing. R Foundation for Statistical Computing, Vienna, Austria. https://www.r-project.org/.

Rash, B. G., and L. J. Richards. 2001. "A Role for Cingulate Pioneering Axons in the Development of the Corpus Callosum." *Journal of Comparative Neurology* 434: 147–157.

Schalbetter, S. M., F. S. Mueller, J. Scarborough, et al. 2021. "Oral Application of Clozapine-N-Oxide Using the Micropipette-Guided Drug Administration (MDA) Method in Mouse DREADD Systems." *Laboratory Animals* 50: 69–75.

Spitzer, S. O., S. Sitnikov, Y. Kamen, et al. 2019. "Oligodendrocyte Progenitor Cells Become Regionally Diverse and Heterogeneous With Age." *Neuron* 101: 459–471.

Stoppini, L., P. A. Buchs, and D. Muller. 1991. "A Simple Method for Organotypic Cultures of Nervous Tissue." *Journal of Neuroscience Methods* 37: 173–182.

Thornton, M. A., and E. G. Hughes. 2020. "Neuron-Oligodendroglia Interactions: Activity-Dependent Regulation of Cellular Signaling." *Neuroscience Letters* 727: 134916.

van der Linden, C. J., P. Gupta, A. I. Bhuiya, et al. 2020. "Olfactory Stimulation Regulates the Birth of Neurons That Express Specific Odorant Receptors." *Cell Reports* 33: 108210.

Walz, A., M. Omura, and P. Mombaerts. 2006. "Development and Topography of the Lateral Olfactory Tract in the Mouse: Imaging by Genetically Encoded and Injected Fluorescent Markers." *Journal of Neurobiology* 66: 835–846.

Wang, C.-L., L. Zhang, Y. Zhou, et al. 2007. "Activity-Dependent Development of Callosal Projections in the Somatosensory Cortex." *Journal of Neuroscience* 27: 11334–11342.

Wosik, K., F. Ruffini, G. Almazan, et al. 2004. "Resistance of Human Adult Oligodendrocytes to AMPA/Kainate Receptor-Mediated Glutamate Injury." *Brain* 127: 2636–2648.

Yamamura, T., J. T. Konola, H. Wekerle, and M. B. Lees. 1991. "Monoclonal Antibodies Against Myelin Proteolipid Protein: Identification and Characterization of Two Major Determinants." *Journal of Neurochemistry* 57: 1671–1680.

Yuan, X., A. M. Eisen, C. J. McBain, and V. Gallo. 1998. "A Role for Glutamate and Its Receptors in the Regulation of Oligodendrocyte Development in Cerebellar Tissue Slices." *Development Cambridge, England* 125: 2901–2914.

Zheng, K., C. Wang, J. Yang, et al. 2018. "Molecular and Genetic Evidence for the PDGFRα-Independent Population of Oligodendrocyte Progenitor Cells in the Developing Mouse Brain." *Journal of Neuroscience: The Official Journal of the Society for Neuroscience* 38: 9505–9513.

Zhou, J., Y. Wen, L. She, et al. 2013. "Axon Position Within the Corpus Callosum Determines Contralateral Cortical Projection." *Proceedings of the National Academy of Sciences* 110: E2714–E2723.

Supporting Information

Additional supporting information can be found online in the Supporting Information section. **Figure S1:** DREADD expression P8. (A) Experimental design. P0 Nex-Cre+ and Nex-Cre− pups were injected with either Gi-DREADD or Gq-DREADD and administered 1 mg/kg CNO from P2–P8. (B) Images of the somatosensory cortex and corpus callosum of Nex-Cre+ pups injected with Gi-DREADD (left) and Gq-DREADD (right) showing m-Cherry (mCh) expression. Green squares represent layer 4 where all cortex images were taken. Images are from P8 pups. Scale bar is 1 mm. (C) cFos staining and quantification in P8 Nex-Cre− and Nex-Cre+ pups injected with DREADD on P0 as indicated. Scale bar is 50 μm. One-way ANOVA Kruskal-Wallis test with multiple comparisons to NexCre− control group. $*p < 0.05$. **Figure S2:** Neuronal activity modulation does not affect OPC proliferation. (A) Experimental design. P0 or P1 NexCre+ or NexCre− mice were injected bilaterally with Gi-DREADD or Gq-DREADD. CNO was fed to all pups from P2–8. Once daily EdU injections were performed on all pups on P5, P6, and P7. Pups were sacrificed for immunohistochemistry at P8. (B) Images from the cortex (top) and corpus callosum (bottom) showing Olig2 and EdU in NexCre−, Gi-DREADD injected and Gq-DREADD injected from left to right. Scale bar is 50 μm (C) quantification of EdU+ Olig2+ cells for Gi-DREADD (left) and Gq-DREADD (right) for the cortex (top) and corpus callosum (bottom). $n = 8–9$ NexCre− pups, 8 Gi-DREADD pups and 7 Gq-DREADD pups. Student's *t*-test. ns, not significant. **Figure S3:** Single cell RNA sequencing quality control data. (A) UMAP embedding showing oligodendrocyte lineage cells from AAV-hM3Di-DREADD injected NexCre+ ($n = 3$ mice pooled) and control NexCre− ($n = 2$ mice pooled) mice all treated with CNO from P0–P8 (peach cluster: OPCs; green cluster: premyelinating cells; purple cluster: mature oligodendrocytes; teal cluster: cycling OPCs). (B) Cell cycle and key cluster markers, (C) percent mitochondrial RNA per cell by cluster (left) and by sample (right). (D) UMIs per cell by cluster (left) and by sample (right). (E) Percent mitochondrial RNA by cluster (left) and by sample (right). (F) Number of unique transcripts detected per cell by cluster (left) and condition (right). **Figure S4:** CNO alone does not affect oligodendrocyte differentiation. (A) Experimental timeline. Cortical slices were prepared from P4 NexCre+ mice. Slices were treated for 48 h from 6-8DIV with CNO or media. (B) Images and quantification of Olig2 along with PDGFRα (OPCs), BCAS1 (premyelinating), and PLP (mature). $n = 4$ animals. Student's *t*-test. ns, not significant. **Figure S5:** AMPA receptors regulate oligodendrocyte differentiation in organotypic cortical slice culture. (A) Schematic of experimental design. NexCre+ pups were taken at P4, and 300 μm thick slices of cortex were plated on a membrane with Gi-DREADD or pAAV-hSyn-DIO-mCherry (control). At 6 and 7DIV, 1 μm CNO alone (control and Gi-DREADD) or 1 μm CNO + 50 μm AMPA (Gi-DREADD + AMPA) was bath applied to slices, and slices were fixed and stained 48 h later at 8DIV. (B) Schematic of slice culture in a dish. Black square represents the area where images

were taken. (C) Images and quantification of PDGFRα (OPCs), BCAS1 (pre-myelinating oligodendrocytes) and PLP (maturing oligodendrocytes) in each experimental condition. Scale bar is 100 μm. $n = 8$ mice. Brown-Forsythe and Welsh ANOVA tests with multiple comparisons to control group. ns, not significant, ***$p < 0.001$, ****$p < 0.0001$. **Table S1:** Gene expression in each cluster. Cluster 0: Gene expression in OPCs; Cluster 1: Gene expression in premyelinating cells; Cluster 2: Gene expression in cycling/proliferating OPCs; Cluster 3: Mature oligodendrocytes. Seurat Wilcoxon Rank sum tests. Adjusted *p* values are Benjamini-Hochberg corrected.